

A novel route to synthesize cubic $\text{ZrW}_{2-x}\text{Mo}_x\text{O}_8$ ($x = 0-1.3$) solid solutions and their negative thermal expansion properties

Ruiqi Zhao^a, Xiaojing Yang^a, Huiliang Wang^a, Jingsa Han^a, Hui Ma^b, Xinhua Zhao^{a,*}

^aCollege of Chemistry, Beijing Normal University, 100875, PR China

^bAnalyzing and Testing Center, Beijing Normal University, 100875, PR China

Received 27 June 2007; received in revised form 5 September 2007; accepted 10 September 2007

Abstract

Cubic $\text{ZrW}_{2-x}\text{Mo}_x\text{O}_8$ (c- $\text{ZrW}_{2-x}\text{Mo}_x\text{O}_8$) ($x = 0-1.3$) solid solutions were prepared by a novel polymorphous precursor transition route. X-ray diffraction (XRD) analysis reveals that the solid solutions are single phase with α - and β - ZrW_2O_8 structure for $0 \leq x \leq 0.8$ and $0.9 \leq x \leq 1.3$, respectively. The optimum synthesis conditions of ZrWMoO_8 are obtained from differential scanning calorimetry–thermal gravimetric analysis (DSC–TGA), XRD and mass loss–temperature/time curves. Following the above experience, the stoichiometric solid solutions of c- $\text{ZrW}_{2-x}\text{Mo}_x\text{O}_8$ ($x = 0-1$) are obtained within 1 wt% of mass loss. The relationships of lattice parameters (a), phase transition temperatures (T_c) and instantaneous coefficients of thermal expansion (α_i) against the content x of Mo are discussed based on the variation of order degree parameters of $\text{ZrW}_{2-x}\text{Mo}_x\text{O}_8$.

© 2007 Published by Elsevier Inc.

Keywords: $\text{ZrW}_{2-x}\text{Mo}_x\text{O}_8$; Polymorphous precursor transition; Synthesis; Negative thermal expansion (NTE)

1. Introduction

Cubic zirconium tungstate (c- ZrW_2O_8) has received considerable interests because of its isotropic negative thermal expansion (NTE) over a wide temperature range (-273 to 777 °C) [1]. Due to the large NTE coefficient, c- ZrW_2O_8 is considered to have potential applications in many fields, especially in those requiring precisely controllable positive, negative or near-zero coefficients of thermal expansion (CTE) composites, such as optical, electronic, engineering and dental-filling applications. However, an order–disorder phase transition of c- ZrW_2O_8 occurs at 155 °C [2], around which there are different CTEs (α is about -9×10^{-6} °C⁻¹ for α - ZrW_2O_8 and -6×10^{-6} °C⁻¹ for β - ZrW_2O_8 [3]). The abrupt change of thermal expansion is disadvantageous for applications if the phase transition temperature (T_c) is included in the

working temperature range. Efforts have been performed to shift T_c either below or above the working temperature range by adjusting the composition of the compound without changing its NTE property. Among the modifications, cubic $\text{ZrW}_{2-x}\text{Mo}_x\text{O}_8$ (c- $\text{ZrW}_{2-x}\text{Mo}_x\text{O}_8$) have been investigated widely [4–8] and T_c is found decreasing with increasing Mo [5,8]. As a representative compound, c- ZrWMoO_8 , whose T_c is as low as -3 °C [7], could be used as an applicable material or as an additive of composite for practical uses above room temperature.

Although there are a variety of methods to synthesize c- ZrW_2O_8 [5,9–15], only two methods have been reported to prepare c- $\text{ZrW}_{2-x}\text{Mo}_x\text{O}_8$ up to date, such as the combustion route [11] and the low-temperature method [4–6]. However both methods are either uncontrollable or time-consuming to obtain phase-pure c- ZrWMoO_8 . Therefore it is very important to find a novel method to synthesize the solid solution conveniently.

In this work, c- ZrWMoO_8 as well as c- $\text{ZrW}_{2-x}\text{Mo}_x\text{O}_8$ ($x = 0-1.3$) solid solutions were synthesized by a novel polymorphous precursor transition route and the crystallographic property, phase transition temperatures and

*Corresponding author. Fax: +86 10 58802075.

E-mail address: xinhua@bnu.edu.cn (X. Zhao).

NTE properties of the synthesized solid solutions were investigated systematically.

2. Experimental section

2.1. Synthesis of $c\text{-ZrW}_{2-x}\text{Mo}_x\text{O}_8$ ($x=0\text{--}1.3$) solid solutions

Starting materials $\text{ZrOCl}_2 \cdot 8\text{H}_2\text{O}$, $(\text{NH}_4)_{10}\text{W}_{12}\text{O}_{41} \cdot 5\text{H}_2\text{O}$ and $(\text{NH}_4)_6\text{Mo}_7\text{O}_{24} \cdot 4\text{H}_2\text{O}$ are analytical-grade reagents. $c\text{-ZrW}_{2-x}\text{Mo}_x\text{O}_8$ ($x=0\text{--}1.3$) were prepared using the procedure described previously [16]. Briefly, the white precipitates were obtained by dropping the solutions of Zr (IV) and Mo (VI) simultaneously into the slurry of W (VI) stoichiometrically for the preparation of $\text{ZrW}_{2-x}\text{Mo}_x\text{O}_8$ ($x=0\text{--}1.3$). The precipitates were dried together with the mother liquor at 100°C and subsequently ground in agate mortar to obtain homogeneous powders. Then the powders were sintered to be precursors at 600°C for 3 h.

After the precursors ($\sim 0.6\text{g}$) were dry-pressed to form cylindrical pellets with a diameter of 10 mm using a steel mould under a pressure of 4 MPa, each pellet was put into a Pt crucible capped with a Pt foil and annealed in a preheated furnace at different temperatures for 1 h. $c\text{-ZrW}_{2-x}\text{Mo}_x\text{O}_8$ ($x=0\text{--}1.3$) were obtained by quenching the heating pellets in ambient atmosphere immediately.

2.2. Measurements

Powder X-ray diffraction (XRD) measurement of samples was carried out using a Philips X-Pert MPD diffractometer. The data were collected from 10° to 90° (2θ), using a step size of 0.0167° (2θ) and the counting time of 20 s per step under 40 kV and 40 mA with $\text{CuK}\alpha$ radiation. The reflections ($2\theta/^\circ$) were calibrated using the line-pair method and indexed using Treor 90 program suited in PowderX software [17]. The lattice parameters were deduced using Unitcell program [18] from the XRD data, which were calibrated with SiO_2 as the internal standard.

Differential scanning calorimetry–thermal gravimetric analysis (DSC–TGA) was performed using SDT Q600 (TA-Instruments) with air flow at a heating rate of 20°Cmin^{-1} , and an open Pt crucible was used as the container. Isothermal mass loss-temperature/time dependence was measured by annealing the pellet of sample either at different temperature for 1 h or in different time at 940°C .

Thermal expansion of ceramic pellets was measured along the ceramic diametrical direction by thermal mechanical analysis (TMA Q400, TA-Instruments) using a macro-expansion quartz probe. The data were collected at a heating rate of 3°Cmin^{-1} from room temperature to 300°C under a constant force of 0.5 N. The temperatures of the minimums of the instantaneous CTE (α_i) versus temperature (T) plot were taken as the order–disorder phase transition temperatures of $\text{ZrW}_{2-x}\text{Mo}_x\text{O}_8$ [2].

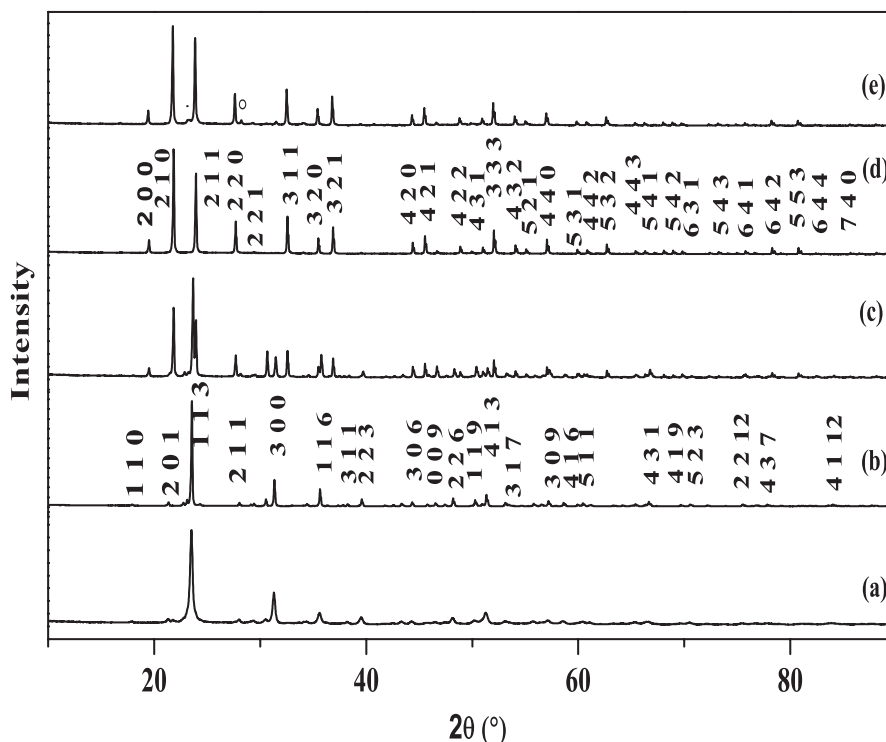


Fig. 1. XRD patterns of (a) the precursor and the precursor calcined for 1 h at (b) 870°C (indexed with trigonal system), (c) 905°C , (d) 913°C (indexed with cubic system), (e) 1150°C (● and ○ denote the reflections of WO_3 and ZrO_2 , respectively).

Calibration of the instrument was performed using an aluminum standard.

3. Results and discussion

3.1. Reaction and transformation of $c\text{-ZrW}_{2-x}\text{Mo}_x\text{O}_8$ ($x = 0\text{--}1.3$) solid solutions

As shown in Fig. 1, the XRD pattern of ZrWMoO_8 precursor (Fig. 1(a)) is identical with that of the precursor calcined at 870°C (Fig. 1(b)). Both of them are indexed with the trigonal crystal system with $a = 9.875 \text{ \AA}$, $c = 17.538 \text{ \AA}$, which is very similar to that of the ZrW_2O_8 trigonal polymorph with the lattice parameters $a = 9.8101(1) \text{ \AA}$, $c = 17.602(2) \text{ \AA}$ [19].

The comparison of XRD patterns between Fig. 1(c) and 1(d) shows that some reflections of $c\text{-ZrWMoO}_8$ appear besides those of trigonal ZrWMoO_8 ($t\text{-ZrWMoO}_8$) when the precursor is calcined at 905°C and single $c\text{-ZrWMoO}_8$ crystallizes completely at 913°C , which can be indexed with the disordered $\beta\text{-ZrW}_2\text{O}_8$ structure with lattice parameter $a = 9.1406(2) \text{ \AA}$ (reference to $a = 9.1400(5) \text{ \AA}$ [11]). According to XRD analysis, the acute endothermic peak in the DSC curve, as shown in Fig. 2, is attributed to the transition from trigonal precursor to $c\text{-ZrWMoO}_8$.

Increasing the sintering temperature above 1050°C , ZrWMoO_8 decomposes to ZrO_2 , WO_3 and MoO_3 , which is revealed from the coexistence of the reflections of $c\text{-ZrWMoO}_8$, ZrO_2 (JCPDS Card no. 83-0951) and WO_3 (JCPDS Card no. 86-1451) as shown in Fig. 1(e). Both the results of the variable temperature DSC–TGA determination (Fig. 2) and isothermal mass-loss measurement at different temperature (Fig. 3(a)) indicate that the mass loss increases drastically when temperature exceeds 1000°C , accompanied with a continuously endothermic process. Considering the absence diffractions of MoO_3 in Fig. 1(e), the mass loss is attributed to the sublimation of MoO_3 .

Preventing the sublimation, namely preventing the decomposition of ZrWMoO_8 , must be beneficial to the

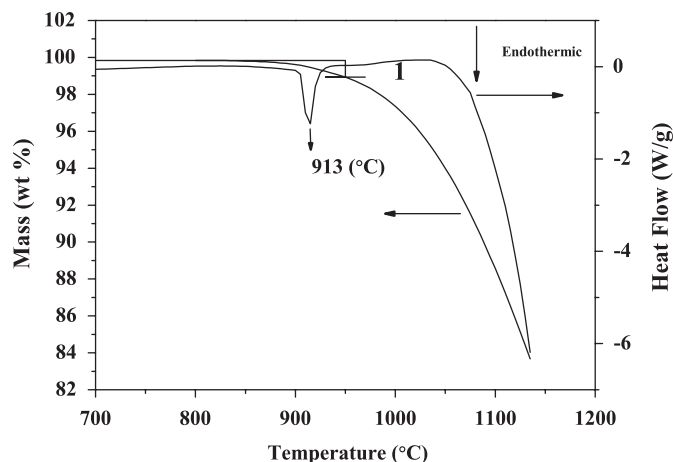


Fig. 2. DSC–TGA curves for the precursor of ZrWMoO_8 .

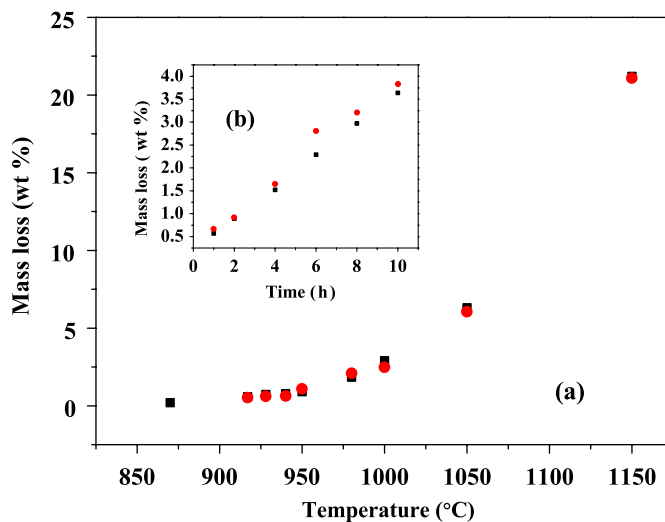


Fig. 3. The mass loss dependence on the temperature of the ZrWMoO_8 pellet: (a) calcined at different working temperatures for 1 h and (b) holding at 940°C for different time.

transformation of the cubic phase. Thus, the key procedure of preparing pure $c\text{-ZrWMoO}_8$ is to optimize heating temperature and holding time to reduce the sublimation of MoO_3 farthest. The time-dependence of mass loss is proportional to the holding time linearly as shown in Fig. 3(b). There is only ca. 1 wt% of continuous mass loss in the temperature range of $870\text{--}950^\circ\text{C}$ as DSC–TGA curves indicated, and less than 1 wt% mass loss within 2 h as the isothermal mass loss temperature/time curves shown. Consequently, phase-pure $c\text{-ZrWMoO}_8$ is prepared beneath 1.8 mol% deviation of the W/Mo ratio between 913 and 950°C within 2 h.

A contrastive experiment was performed by calcining the mixture of ZrO_2 , MoO_3 and WO_3 in $910\text{--}950^\circ\text{C}$ for 1 h, but pure $c\text{-ZrWMoO}_8$ can't be obtained. Increasing sintering temperature to 980°C and prolonging the holding time to 3 h, nominal cubic ZrWMoO_8 accompanied with trace ZrO_2 and WO_3 can be formed. Therefore, it can be concluded that the formation of the polymorphous precursor stabilizes MoO_3 from sublimating and is beneficial to prepare the stoichiometrically cubic solid solutions.

Fig. 4 shows the XRD patterns of the precursors ($x = 0\text{--}1.3$), which can be classified into two kinds of substances. For $x = 0.2\text{--}1.3$, most reflections can be assigned to $t\text{-ZrW}_{2-x}\text{Mo}_x\text{O}_8$ and therefore the process of preparing $c\text{-ZrW}_{2-x}\text{Mo}_x\text{O}_8$ is similar to that of $c\text{-ZrWMoO}_8$. However the precursors with low x contain large amounts of amorphous phase, although there are some distinct reflections in the XRD patterns. The amorphous precursors convert to the mixture of ZrO_2 , WO_3 and MoO_3 rather than $t\text{-ZrW}_{2-x}\text{Mo}_x\text{O}_8$ after calcination for 3 h in $700\text{--}900^\circ\text{C}$. Further increasing the temperature up to 1160°C and holding the annealing time for 1 h, the precursor of $\text{ZrW}_{1.9}\text{Mo}_{0.1}\text{O}_8$ is also converted to the cubic phase instead of to the trigonal phase.

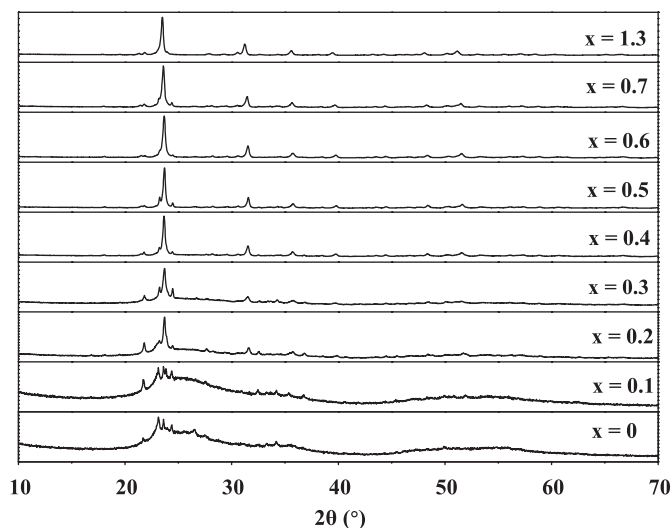


Fig. 4. The XRD patterns of the precursors ($x = 0-1.3$).

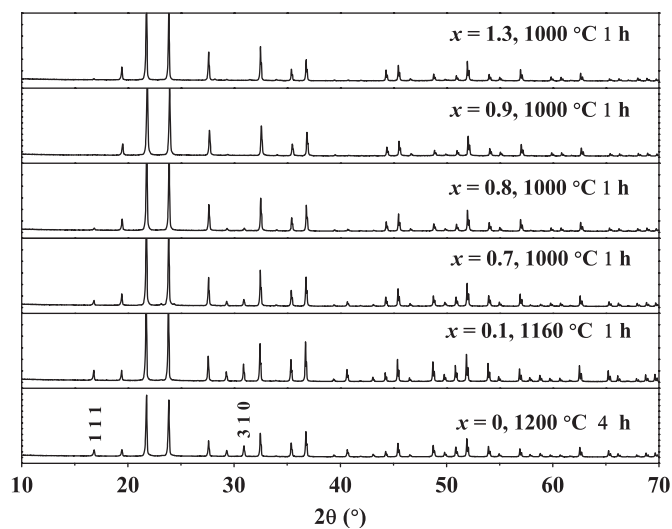


Fig. 5. The XRD patterns of $c\text{-ZrW}_{2-x}\text{Mo}_x\text{O}_8$. The content x of Mo and the preparation conditions are displayed on the pattern. The indexes of reflections are indexed with the $\alpha\text{-ZrW}_2\text{O}_8$ structure.

The process of transition from trigonal precursors to pure $c\text{-ZrW}_{2-x}\text{Mo}_x\text{O}_8$ is analogous to that of $c\text{-ZrW}\text{MoO}_8$. The optimal couple of temperature and time emerges through experiments and the phase-pure solid solutions of nominal $c\text{-ZrW}_{2-x}\text{Mo}_x\text{O}_8$ ($x = 0-1.3$) are synthesized. The XRD patterns and the synthesis conditions are displayed in Fig. 5. In these conditions, mass loss is less than 1 wt% except for the Mo-rich solid solutions ($x > 1$). We note that there is a close relation between the synthesis temperature and the content x of Mo in solid solutions. Compared with $c\text{-ZrW}_2\text{O}_8$ [20], the synthesis temperature of pure $c\text{-ZrW}_{2-x}\text{Mo}_x\text{O}_8$ decreases markedly with the introduction of Mo. Beyond $x = 1$, the synthesis temperatures reverse to higher temperature and result in more mass loss. For those with $x > 1.3$, no pure $c\text{-ZrW}_{2-x}\text{Mo}_x\text{O}_8$ is obtained by the present method.

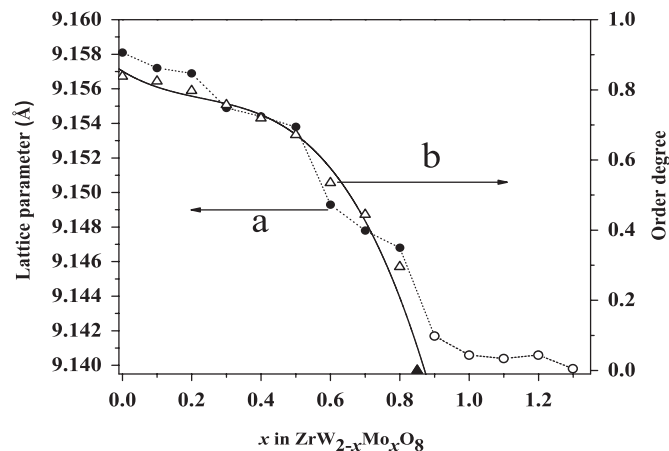


Fig. 6. The relations of (a) lattice parameter and (b) order degree of $c\text{-ZrW}_{2-x}\text{Mo}_x\text{O}_8$ versus the content x of Mo. (●): the ordered; and (○): disordered structure type. (△): order degree (▲ represents the extrapolated order degree from linear equation displayed in Fig. 8).

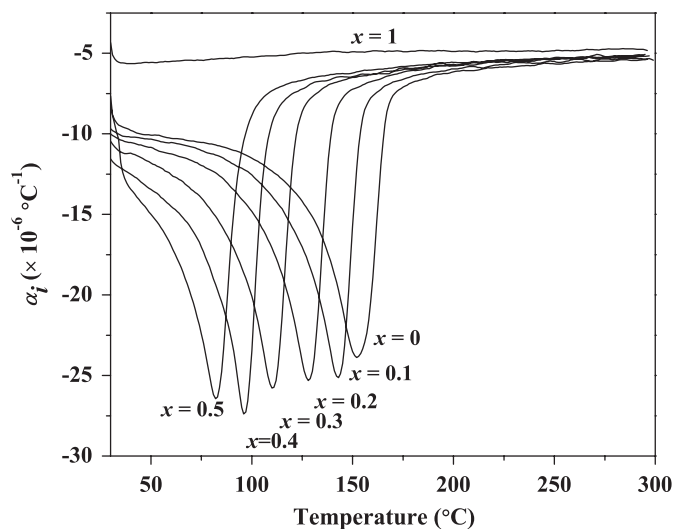


Fig. 7. The dependence of instantaneous coefficient of thermal expansion (α_t) of $c\text{-ZrW}_{2-x}\text{Mo}_x\text{O}_8$ on temperature.

3.2. Lattice parameters and the order degrees of $c\text{-ZrW}_{2-x}\text{Mo}_x\text{O}_8$ ($x = 0-1.3$) solid solutions

From the patterns shown in Fig. 5, $c\text{-ZrW}_{2-x}\text{Mo}_x\text{O}_8$ can be indexed with the ordered $\alpha\text{-ZrW}_2\text{O}_8$ structure (S.G.: $P2_13$) for $x = 0-0.8$ and disordered $\beta\text{-ZrW}_2\text{O}_8$ structure (S.G.: $Pa\bar{3}$) for $x = 0.9-1.3$ [1,2]. As shown in Fig. 6, the lattice parameters a of $\alpha\text{-ZrW}_{2-x}\text{Mo}_x\text{O}_8$ ($x = 0-0.8$) shrink markedly with the introduction of Mo. Meanwhile, the relative intensity of reflection 310 gradually decreases, as shown in Fig. 5, implying that the order degree (ω) of $\alpha\text{-ZrW}_{2-x}\text{Mo}_x\text{O}_8$ ($x = 0-0.8$) is reduced with increase x [6,21,22].

According to Bragg-Williams approximation [23],

$$\frac{T}{T_c} = \frac{2\omega}{\ln(1 + \omega/1 - \omega)} \quad (1)$$

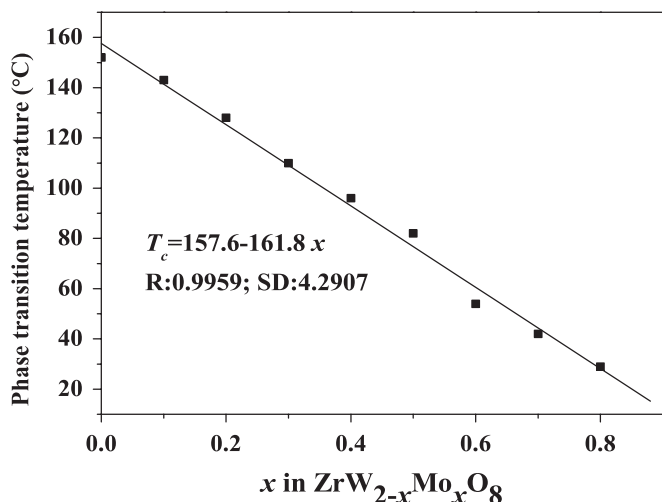


Fig. 8. The dependence of phase transition temperatures T_c on the content x of $c\text{-ZrW}_{2-x}\text{Mo}_x\text{O}_8$.

the order degree (ω) of a given $\alpha\text{-ZrW}_{2-x}\text{Mo}_x\text{O}_8$ at room temperature (supposing $T = 293\text{ K}$) can be deduced from its phase transition temperature (T_c , which is correlated with content x of Mo), which is determined by TMA curves as shown in Fig. 7. Based on the experimental results, the dependence of ω on x is established in Fig. 6, which is fitted well with polynomial function and the value of content x with $\omega = 0$ is extrapolated to be 0.87, which is consistent with the value deduced from linear equation displayed in Fig. 8. The similar trends of both lattice parameter and order degree parameter on content x appear in Fig. 6 obviously and a correlation between them emerges.

For $x = 0.9\text{--}1.3$, $\text{ZrW}_{2-x}\text{Mo}_x\text{O}_8$ is indexed with the $\beta\text{-ZrW}_2\text{O}_8$ structure and the lattice parameters are $a = 9.1417\text{ \AA}$ and 9.1406 \AA for $x = 0.9$ and 1 , respectively, in which the latter value is comparable to the reported lattice parameter of ZrWMoO_8 ($9.1400(5)\text{ \AA}$) [11]. Over the content $x = 1$, little change of lattice parameters are observed for nominal $\text{ZrW}_{2-x}\text{Mo}_x\text{O}_8$ ($x = 1.1, 1.2, 1.3$). Apparently, the real concentration of Mo in the presented $\text{ZrW}_{2-x}\text{Mo}_x\text{O}_8$ does not exceed 1. Considering the higher synthesis temperature, the deviation from the nominal composition is explicable.

3.3. Phase transition temperatures and NTE properties of $c\text{-ZrW}_{2-x}\text{Mo}_x\text{O}_8$

The plot of $\alpha_i T$ and the dependence of T_c on x of $\text{ZrW}_{2-x}\text{Mo}_x\text{O}_8$ are shown in Figs. 7 and 8, respectively. As shown in Fig. 7, above T_c , α_i of all $\beta\text{-ZrW}_{2-x}\text{Mo}_x\text{O}_8$ is almost close to about $-5 \times 10^{-6}\text{ }^\circ\text{C}^{-1}$. On the other hand, α_i of $\alpha\text{-ZrW}_{2-x}\text{Mo}_x\text{O}_8$ approaches to about $-10 \times 10^{-6}\text{ }^\circ\text{C}^{-1}$ at the temperatures far below T_c . The values of α_i are adjacent with the average linear CTEs (α_a) of $\beta\text{-ZrW}_2\text{O}_8$ ($-6 \times 10^{-6}\text{ }^\circ\text{C}^{-1}$) and $\alpha\text{-ZrW}_2\text{O}_8$ (about $-9 \times 10^{-6}\text{ }^\circ\text{C}^{-1}$) [3] at the same temperature ranges where ω equals to zero or 1, respectively. However, when T drawing near T_c the α_i of $\alpha\text{-ZrW}_{2-x}\text{Mo}_x\text{O}_8$ drops down

rapidly and the order degree parameter ω which can be deduced from Eq. (1) decreases synchronously. By the same reasoning, $\alpha\text{-ZrW}_{2-x}\text{Mo}_x\text{O}_8$ at room temperature with different α_i would also be rationalized.

The dependence of T_c on the levels x of Mo is fitted linearly. T_c of ZrWMoO_8 is obtained by extrapolating the fitted line on $-4.2\text{ }^\circ\text{C}$, which is consistent with $-3\text{ }^\circ\text{C}$ [7]. The downtrend of T_c depending on x can be understood from the viewpoint that there are different bond strengths for Mo–O and W–O, respectively. With more introduction of weaker bond Mo–O, the reversal of adjacent MO_4 tetrahedrons becomes easier [2].

4. Conclusions

A series of $c\text{-ZrW}_{2-x}\text{Mo}_x\text{O}_8$ ($x = 0\text{--}1.3$) solid solutions were successfully synthesized by the polymorphous precursor transition route. The optimum combination of annealing temperature and holding time are summed up from experiments. Under these conditions, stoichiometric solid solutions are synthesized within 1 wt% of mass loss. At room temperature, $c\text{-ZrW}_{2-x}\text{Mo}_x\text{O}_8$ adopt the α - ($x = 0\text{--}0.8$) and β - ($x = 0.9\text{--}1.3$) ZrW_2O_8 structures, respectively. The lattice parameters (a) and phase transition temperatures (T_c) of $\alpha\text{-ZrW}_{2-x}\text{Mo}_x\text{O}_8$ decrease with increasing x . As temperature approaches T_c , the instantaneous CTE (α_i) of $\alpha\text{-ZrW}_{2-x}\text{Mo}_x\text{O}_8$ decrease rapidly with increasing temperature. This trend agrees well with the α_i dependence on the content x of $\alpha\text{-ZrW}_{2-x}\text{Mo}_x\text{O}_8$ at the same temperatures. However, α_i vary slightly at the temperatures far away from T_c , where the order degree of $c\text{-ZrW}_{2-x}\text{Mo}_x\text{O}_8$ closes to 1 or zero.

Acknowledgments

This work was supported by a grant from the National Science Foundation of China: NSFC 20471010 and the Foundation of Beijing Key Discipline of Inorganic Chemistry. And we are also grateful to the laboratory of TA Instruments-Waters LLC in Beijing for their help in DSC–TGA.

References

- [1] T.A. Mary, J.S.O. Evans, T. Vogt, A.W. Sleight, *Science* 272 (1996) 90–92.
- [2] J.S.O. Evans, T.A. Mary, T. Vogt, M.A. Subramanian, A.W. Sleight, *Chem. Mater.* 8 (1996) 2809–2823.
- [3] S. Allen, J.S.O. Evans, *Phys. Rev. B* 68 (2003) 134101.
- [4] L. Huang, Q.G. Xiao, H. Ma, G.B. Li, F.H. Liao, Ch.M. Qi, X.H. Zhao, *Eur. J. Inorg. Chem.* 22 (2005) 4521–4526.
- [5] C. Closmann, A.W. Sleight, J.C. Haygorth, *J. Solid State Chem.* 139 (1998) 424–426.
- [6] S.R. Guo, X.B. Deng, H. Ma, X.H. Zhao, *Chem. J Chinese U.* 28 (2007) 410–414.
- [7] J.S.O. Evans, P.A. Hanson, R.M. Ibberson, N. Duan, U. Kameswari, A.W. Sleight, *J. Am. Chem. Soc.* 122 (2000) 8694–8699.
- [8] S.Y. Zhang, X.H. Zhao, H. Ma, *Chinese J. Chem.* 18 (4) (2000) 571–575.

- [9] L.L.Y. Chang, M.G. Scroger, B. Phillips, *J. Am. Ceram. Soc.* 50 (1967) 211.
- [10] C. Martinek, F.A. Hummel, *J. Am. Ceram. Soc.* 51 (1968) 227.
- [11] U. Kameswari, A.W. Sleight, J.S.O. Evans, *Int. J. Inorg. Mater.* 2 (2000) 333–337.
- [12] C. Lind, A.P. Wilkinson, *J. Sol–Gel Sci. Technol.* 25 (2002) 51–56.
- [13] C.D. Meyer, I.V. Driessche, S. Hoste, *Key Eng. Mater.* 206–213 (2002) 11–14.
- [14] X.B. Deng, X.H. Zhao, J.S. Han, *Chinese J. Inorg. Chem.* 21 (9) (2005) 1357–1362.
- [15] P.D. Yang, D.Y. Zhao, D.I. Margolese, B.F. Chmelka, G.D. Stucky, *Nature* 396 (1998) 152–155.
- [16] X.H. Zhao, R.Q. Zhao, Chinese Patent, CN: 1850721A.
- [17] C. Dong, *J. Appl. Crystallogr.* 32 (1999) 838.
- [18] T.J.B. Holland, S.A.T. Redfern, *Mineral. Mag.* 53 (1997) 305–314.
- [19] L.D. Noailles, H.H. Peng, J. Starkovich, B. Dunn, *Chem. Mater.* 16 (2004) 1252–1259.
- [20] A.W. Sleight, T.A. Mary, J.S.O. Evans, US Patent No. 5514360, 1995.
- [21] N. Nakajima, Y. Yamamura, T. Tsuji, *Solid State Commun.* 128 (2003) 193–196.
- [22] H.H. Li, J.S. Han, H. Ma, L. Huang, X.H. Zhao, *J. Solid State Chem.* 180 (2007) 852–857.
- [23] M. Plischke, B. Bergersen, *Equilibrium Statistical Physics*, Prentice-Hall, Inc, Englewood Cliffs, NJ, 1989, p. 66.